IEEE Access
Multidisciplinary | Rapid Review | Open Access Journal

Received March 8, 2021, accepted April 1, 2021, date of publication April 9, 2021, date of current version April 19, 2021.

Digital Object Identifier 10.1109/ACCESS.2021.3072150

Localization Method for Implant Devices Using Electromagnetic Scattering Based on Sparse Reconstruction

TAKAHIRO ITO[1], (Member, IEEE), DAISUKE ANZAI[2], (Member, IEEE), JIANQING WANG[2], (Fellow, IEEE), AND HIROKAZU TAKANA[1], (Senior Member, IEEE)

[1]Department of Medical Information Sciences, Hiroshima City University, Hiroshima 731-3194, Japan
[2]Department of Electrical and Mechanical Engineering, Nagoya Institute of Technology, Nagoya 466-8555, Japan

Corresponding author: Takahiro Ito (ito-t@hiroshima-cu.ac.jp)

This research was supported by the Ministry of Internal Affairs and Communications/Strategic Information and Communications R&D Promotion Programme (MIC/SCOPE) #185106002.

ABSTRACT Herein, we propose a localization method for implant devices using electromagnetic scattering based on sparse reconstruction. We define the product of the total electric field and the complex relative permittivity as a new unknown variable, which is expected to be sparse. Computer simulations are conducted to validate the sparsity of the estimated variable, and localization errors are evaluated to confirm the performance improvement using the sparsity-based localization method. The result confirmed the excellent localization performance, particularly below 17 MHz, even under low signal-to-noise power ratios.

INDEX TERMS Electromagnetic scattering, implant medical device, localization, sparsity.

I. INTRODUCTION

In the field of medical treatment and healthcare, body area networks (BANs) have garnered considerable attention [1]–[3]. Wireless capsule endoscopy (WCE), which involves a small pill comprising a transmitter, camera, and battery, is a typical application of BANs [4], [5]. The pill used in WCE is swallowed by a patient, captures photographs of the gastrointestinal tract, and then transmits them to receivers on the patient's waist. Knowledge regarding locations to perform WCE in the human body can facilitate doctors in diagnosing diseases and identify tumor locations; therefore, many location estimation methods for WCE have been investigated. In addition to WCE, location information is useful for any other BAN application device.

Many localization techniques using BANs have been investigated. For example, ultrawideband (UWB)-ranging-based localization has garnered attention [6], [7]. When a node is worn on the human body, UWB ranging enables the node location to be estimated with high accuracy owing to its high spatial resolution. Meanwhile, the propagation of electromagnetic (EM) waves for the localization of implant devices differs from that for the localization of wearable devices. In particular, the signal transmitted from implant devices is attenuated considerably by the human body; therefore, the implant propagation channels must be investigated via experiments and EM analyses to optimize a localization problem for the implant channels [8], [9]. Localization methods using the received signal strength indicator or time of arrival from transmitted signals have been proposed; it has been reported that those methods can yield accurate estimations of implant device locations [5], [10], [11]. Meanwhile, localization methods based on EM scattering [12], [13] can be applied to all implant medical devices, including those without wireless communication; however, the attainable estimation accuracy remains low because of the large number of unknown variables.

Generally, localization based on EM scattering involves an ill-posed problem because the number of receivers is small compared with the number of unknown variables, such as the electric constant distribution of the human body. To solve this inverse problem, the Moore-Penrose inverse matrix [14] is often used. This method is effective for human body structure estimation [15]; however, it might not be suitable for implant device localization problems. Implant devices contain metal parts; therefore, their electric constant differ

The associate editor coordinating the review of this manuscript and approving it for publication was Lorenzo Mucchi.

significantly from that of human biological tissues. The solution obtained using the Moore-Penrose inverse matrix is an L2 norm minimized solution. This implies that the solution does not exhibit a significant contrast, e.g., the combination of human tissues and metal. Although the Moore-Penrose inverse solution can elucidate the observed scattered electric field effectively, it incurs a significant error when estimating the electric constant distribution.

Herein, we propose a location estimation algorithm for implant devices, focusing on the sparsity of the product of electric constants and the electric field in the human body. In this study, sparsity implies that most of the elements are zero and that only a few elements are non-zero; this concept is widely used in signal processing algorithms [16], [17]. Based on a frequency of 30 MHz [12], we previously confirmed that the distribution of the abovementioned product exhibited sparsity. When the frequency increased, the electric field in the deep area decreased; hence, scattering by metal decreased accordingly. This result implies that the scattering field components by the metal will be difficult to observe at antennas located outside the body. However, if the employed frequency is lower, then a larger antenna is required. In this study, we determined the optimized frequency that can be used to estimate the implant device location with high accuracy based on sparsity using computer simulations.

The remainder of the paper is organized as follows: Section 2 presents the theory of EM wave scattering, and Section 3 describes the location estimation algorithm using the scattered electric field based on sparsity. The sparsity of the product of the electric field and complex relative permittivity is validated in Section 4; additionally, the localization performance based on computer simulation is presented. Finally, Section 5 concludes the paper.

II. ELECTROMAGNETIC SCATTERING ON HUMAN BODY

The system model is illustrated in Fig. 1. A transverse-magnetic-mode plane wave is irradiated in the y-direction toward the human body. Assuming that the human body is a set of regularly arranged infinitely long cylinders, we can consider the localization problem as a two-dimensional problem. The analysis area was a plane that included part of the small intestine. The receiver antennas were placed around the human body to observe both the incident wave and the waves scattered by the human body, i.e., including the implant device.

M receivers located around the human body was used to observe the sum of the incident electric fields $\boldsymbol{e}^i$ and the scattered fields $\boldsymbol{e}^s$.

$$\boldsymbol{e} = \boldsymbol{e}^i + \boldsymbol{e}^s \tag{1}$$

where $\boldsymbol{e}$ is the total electric field. Hence, the scattered field can be obtained as the difference between the observed total field and the incident field. Fig. 2 shows the analysis model. The human body was partitioned into areas measuring 0.01 m × 0.01 m. The dielectric constants of each biological

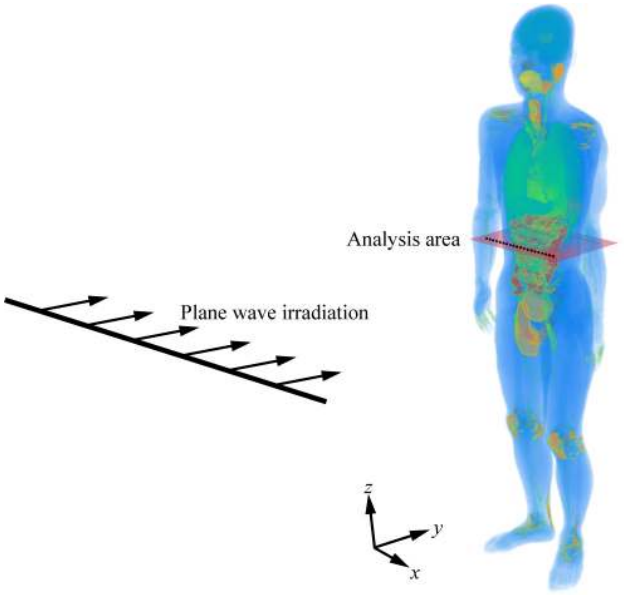

FIGURE 1. Implant device localization system. Black dots on the analysis area imply receivers.

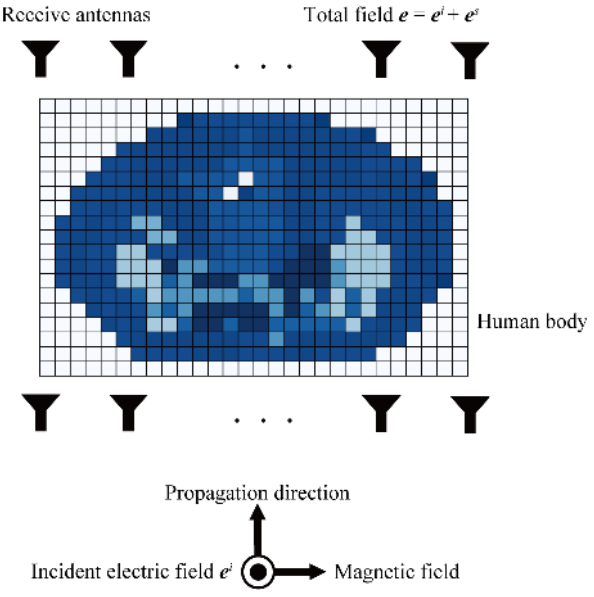

FIGURE 2. Analysis model in x-y plane. Receivers are placed around the body.

tissue at the employed frequency [18] were assigned to each cell.

Using the method of moments, the total fields on each cell can be expressed by the following equations [15], [19]:

$$\boldsymbol{e} = (AT + I)^{-1}\boldsymbol{e}^i \tag{2}$$

Here, A is an $N \times N$ matrix, whose components are

$$A_{m,n} = \begin{cases} (j/2)\{\pi k r_n H_1^{(2)}(kr_n) - 2j & (m = n) \\ (j\pi k r_n/2) J_1(kr_n) H_0^{(2)}(k\rho_{m,n}) & (m \neq n) \end{cases} \tag{3}$$

where k, r_n, and $\rho_{m,n}$ are the wave number, radius of the n-th cell, and distance between the m-th and n-th cells,

respectively. $H_\nu^{(n)}$ is the n-th-kind Hankel function of the ν-th order, and J_ν is the Bessel function of the ν-th order. T is an $N \times N$ matrix whose diagonal elements are

$$T_{n,n} = \varepsilon_r(n) - j\frac{\sigma(n)}{\omega\varepsilon_0} - 1 \tag{4}$$

where $\varepsilon_r(n)$, $\sigma(n)$, ω, and ε_0 are the relative permittivity of the n-th cell, conductivity of the n-th cell, angular frequency of the incident plane wave, and relative permittivity of free space, respectively. The scattered fields observed at the receivers are the superposition of scattering from all cells, as follows:

$$\boldsymbol{e}^s = BE\boldsymbol{\tau} \tag{5}$$

where B is an $M \times N$ matrix, whose components are expressed as

$$B_{m,n} = -(j\pi k r_n/2)J_1(kr_n)H_0^{(2)}(k\rho'_{m,n}). \tag{6}$$

E is an $N \times N$ diagonal matrix whose diagonal components are the total fields $\boldsymbol{e}$. $\boldsymbol{\tau}$ is an $N \times 1$ vector, which contains the diagonal entries of T. $\rho'_{m,n}$ is the distance between the m-th receiver and the n-th cell.

III. LOCALIZATION METHOD BASED ON SPARSITY

A. APRINCIPLE OF EM SCATTERING-BASED LOCALIZATION

In EM imaging techniques, the internal human body structure, namely, the distribution of the electric constant $\boldsymbol{\tau}$ in (5), is calculated. If the correct $\boldsymbol{\tau}$ is obtained, then the location of the implant device is regarded as the cell location with the largest conductivity because the implant device is composed primarily of metals, such as transmitters and batteries. As mentioned above, the internal structure estimation by the L2 norm minimization using the Moore-Penrose inverse matrix is not suitable for solving this problem.

In this study, we applied a sparse vector reconstruction algorithm [20], [21] to the implant device localization problem. A sparse solution can express the contrast between biological tissues and metals. Generally, the L0 norm minimization is required to obtain a sparse solution. However, assuming that only one implant device is implanted into the body, the sparse vector can be reconstructed using a greedy algorithm with only one iteration instead of using the L0 norm minimization.

B. LOCALIZATION ALGORITHM BASED ON SPARSE VECTOR RECONSTRUCTION

We estimated the product of E and $\boldsymbol{\tau}$ in (5) as the unknown variable, which is defined as $\boldsymbol{\epsilon}$ herein. Therefore, (5) can be rewritten as

$$\boldsymbol{e}^s = B\boldsymbol{\epsilon}. \tag{7}$$

It is noteworthy that (7) is a typical sparse equation, where $\boldsymbol{\epsilon}$ can be assumed to be a sparse vector. We can determine $\boldsymbol{\epsilon}$ by solving the sparse reconstruction problem in (7).

TABLE 1. Localization algorithm based on sparse reconstruction.

Initialize: $= 0$
Measured scattered field: $\boldsymbol{e}^s = \boldsymbol{e} - \boldsymbol{e}^i$
Column vector of B: $B = [\boldsymbol{B}_1\, \boldsymbol{B}_2 \cdots \boldsymbol{B}_N]$
for $i = 1, \ldots, N$
$c(i) = \mathrm{corrcoef}(\boldsymbol{e}_S, \boldsymbol{B}_i)$
Index of maximum: $i^{\mathrm{est}} = \arg\max_i c(i)$
Estimated location: $i^{\mathrm{est}} \rightarrow (x^{\mathrm{est}}, y^{\mathrm{est}})$
Reconstruct vector: $_i = \frac{\lvert \boldsymbol{e}^s \rvert}{\lvert \boldsymbol{B}_i \rvert}$

The reconstruction algorithm is listed in Table 1. During the initialization, $\boldsymbol{\epsilon}$ was set to a zero vector. Subsequently, the correlation coefficients of the scattered field $\boldsymbol{e}^s$ and each column vector of B were calculated. The implant device location was determined by the index of the cell that had the highest correlation coefficient. Finally, $\boldsymbol{\epsilon}$ was reconstructed by updating the element in the estimated index.

IV. PERFORMANCE EVALUATION

A. VALIDATION OF SPARSITY

The scattered and total fields were calculated to validate the sparsity of the estimator. A numerical human body model developed by the National Institute of Information and Communications Technology (NICT) [22] was used. The analysis area was the x-y plane, where the height was 1.06 m from the ground. The implant device was located in a shallow and deep area of the human body, as illustrated in Fig. 3. Ten receivers were located in front of and behind the body. It is noteworthy that ten receivers should be accepted in real-world implant device applications because more than five receivers are placed on one side of the human body in general capsule endoscopy [23]. The incident wave source was located 1 m away from the body. The frequency of the incident plane wave was set to 30, 150, and 400 MHz.

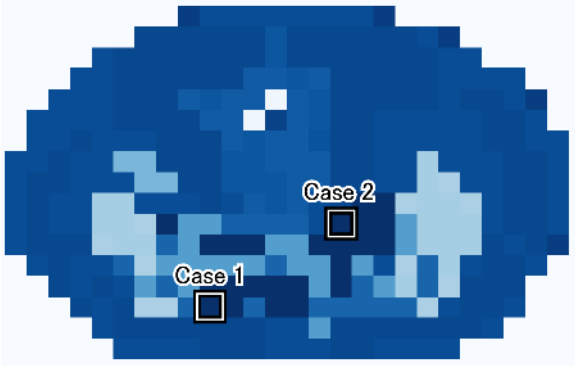

FIGURE 3. Implant device locations in the simulation. Case 1 is the situation that the implant device is placed close to the body surface, and Case 2 is placed on deep location.

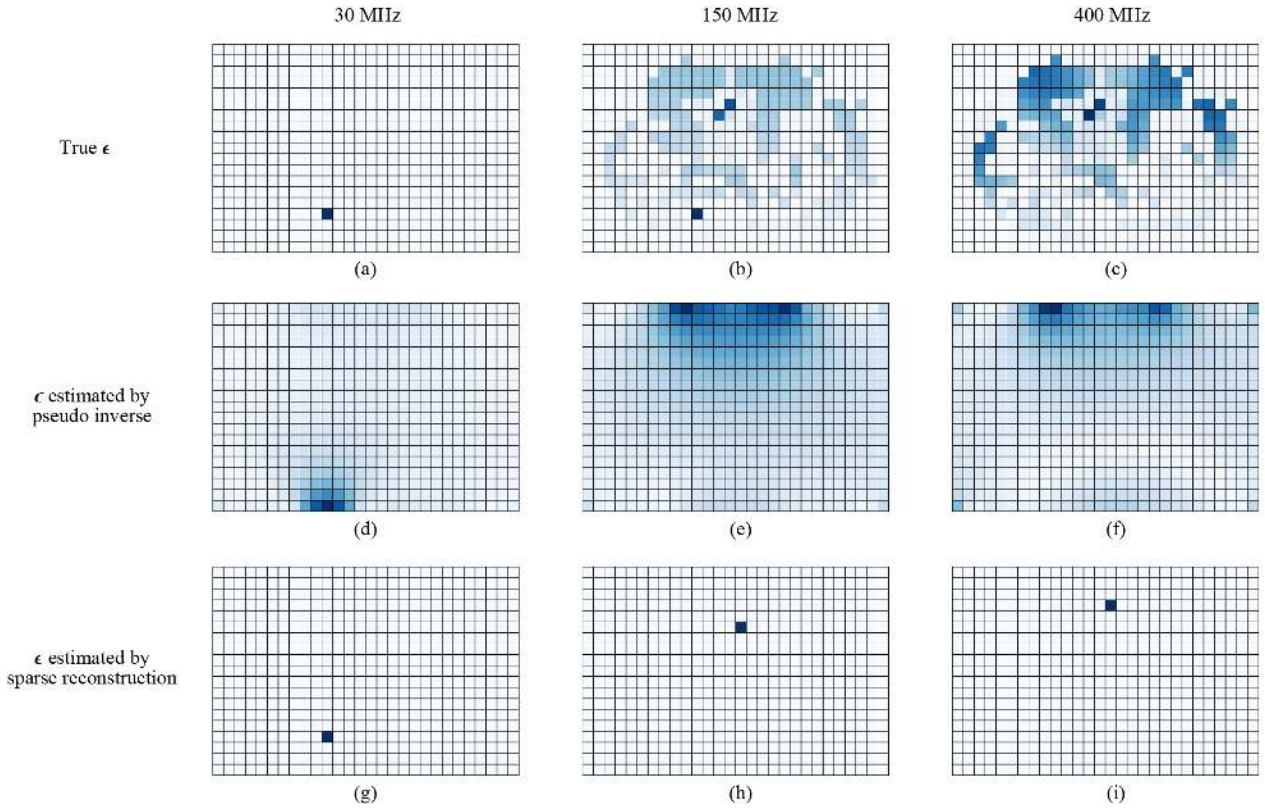

FIGURE 4. Visualized distribution of (a-c) True ϵ (d-f) ϵ estimated by pseudo inverse matrix (g-i) ϵ estimated by sparse reconstruction in Case 1 with employed frequency of 30, 150, 400 MHz, respectively.

Subsequently, $\boldsymbol{\epsilon}$ was estimated using the Moore-Penrose inverse matrix and the proposed method described in Section 3, separately. Figs. 4 and 5 show the true and estimated $\boldsymbol{\epsilon}$ for each case, respectively. When the employed frequency was 30 MHz, only one cell exhibited a large value, whereas the others exhibited values of approximately zero even when the implant device was located in a deep area, as shown in Fig. 5 (a). At the other employed frequencies of 150 and 400 MHz, sparsity on $\boldsymbol{\epsilon}$ was no longer observed. The solution estimated by the pseudo inverse matrix was a blur distribution, rendering it difficult to estimate the implant device location accurately. In our proposed method, the sparse solution can be obtained easily, as shown in Fig. 4 (g); however, the localization error remained significant at the employed frequencies of 150 and 400 MHz. The collapse of sparsity is one of the reasons that caused the localization error. However, an increase in the number of receivers can prevent the collapse of sparsity; hence, the localization error can be reduced using our proposed method.

B. LOCALIZATION PERFORMANCE

It is important to consider potential problems associated with the localization of implants. In a real environment, various types of interferences should be superimposed on the observed electric fields, such as noise emitted from the power supply unit of medical equipment and radio services [24]–[26]. These interferences significantly affect the localization of implants. However, in some cases, interference can be considered as an acceptance level. For example, in [25], the measured interference in a real scenario reached 82 dBuV/m, which is much smaller than the interference of general noise sources, i.e., thermal noise generated in the amplifier of the receiver.

The localization performances of the two methods were evaluated. The implant device was located at one cell inside the small intestine; hence, computer simulations with 24 patterns of each implant device location were conducted. The frequency was set from 1 to 400 MHz. The average localization errors are shown in Fig. 6. By the pseudo inverse, whereas the localization error was achieved at 0.055 m at low frequencies, the localization error worsened as the frequency increased because clear sparsity characteristics were difficult to achieve. Meanwhile, the proposed method with sparse reconstruction and localization error yielded a much better accuracy compared with the pseudo-inverse method. In particular, at frequencies below 17 MHz, error-free localizations were achieved.

The localization performance when noise was superimposed on the observed scattered fields is shown in Fig. 7. When the signal-to-noise power ratio (SNR) was set to 30 dB, the localization error was approximately 0.006 m at employed frequencies of 10 and 17 MHz. To reduce the localization error to less than 0.02 m, which is approximately the diameter of the small intestine, the SNR should be at least 25 dB at

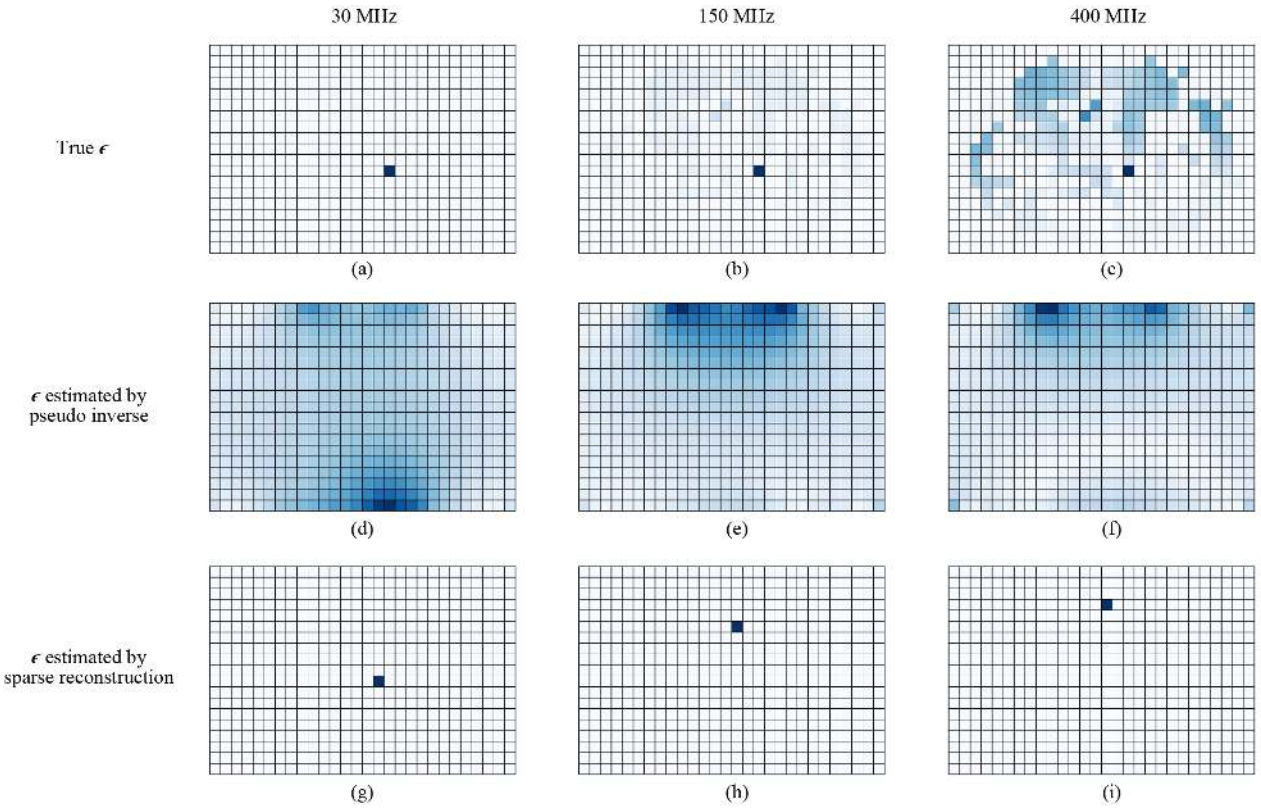

FIGURE 5. Visualized distribution of (a-c) True ϵ (d-f) ϵ estimated by pseudo inverse matrix (g-i) ϵ estimated by sparse reconstruction in Case 2 with employed frequency of 30, 150, 400 MHz, respectively.

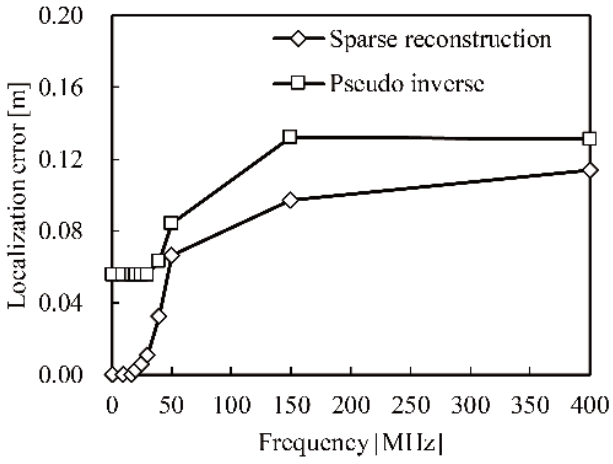

FIGURE 6. Average localization error with the employed frequency of from 1 MHz to 400 MHz.

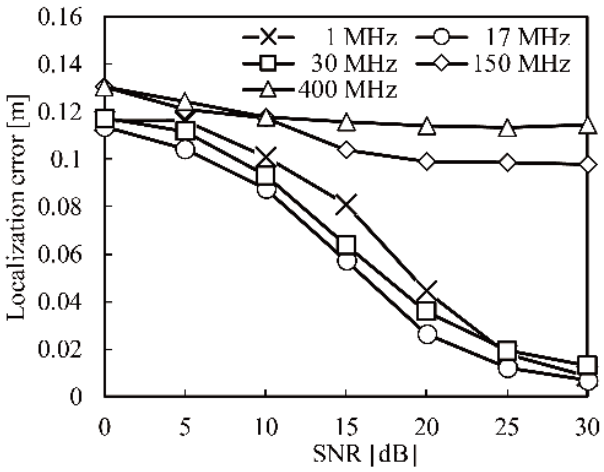

FIGURE 7. Localization error with Gaussian noise.

a frequency of less than 30 MHz. Assuming a bandwidth of 300 kHz (MICS band) and a room temperature of 300 K, the thermal noise power was approximately −119 dBm; therefore, an SNR of 25 dB may be feasible in realistic cases.

Fig. 8 illustrates the dependency of the number of receivers on the localization performance when the SNR was 30 dB. The simulation results show that the localization performance can be improved using a large number of receivers at frequencies of 17 and 30 MHz. For example, the localization errors at 17 and 30 MHz converged within 0.004 and 0.008 m, respectively. For frequencies 150 and 400 MHz, the converged localization error remained large even as the number of receivers increased. This implies that it is important to not only increase the number of receivers, but also to select the appropriate frequency for sparse reconstruction.

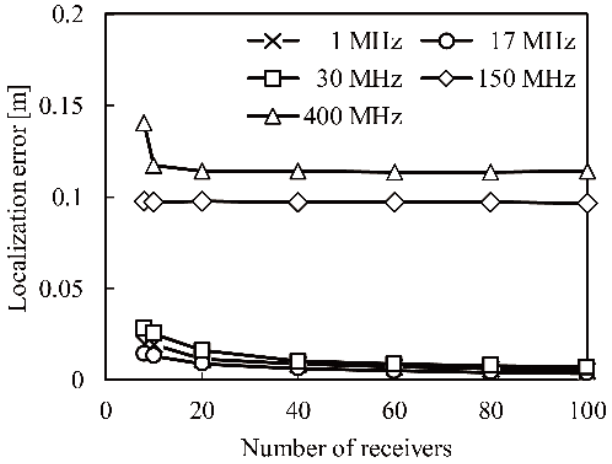

FIGURE 8. Dependency of the number of receivers with SNR = 30 dB.

V. CONCLUSION

A sparsity-based localization algorithm for implant devices was proposed herein. We confirmed that clear sparsity characteristics appeared on the product of the complex relative permittivity and the total electric field at frequencies less than 30 MHz. A computer simulation for localization performance evaluation was conducted using a numerical human body model. The results indicated a good localization error at a frequency below 17 MHz. If the employed frequency is 30 MHz, then an SNR of at least 25 dB is required to achieve a localization error of 0.02 m. Furthermore, it was confirmed that more receivers resulted in better localization performance at frequencies of 17 and 30 MHz, where a localization error of within 0.01 m was achieved when the numbers of receivers were 20 and 40, respectively. However, the employed frequency must be appropriate for sparse reconstruction, e.g., less than 30 MHz. For future studies, we plan to perform an experimental evaluation of the proposed localization method to validate its efficiency in a real environment.

REFERENCES

[1] J. Wang and Q. Wang, *Body Area Communications: Channel Modeling, Communication Systems, and EMC*. Hoboken, NJ, USA: Wiley, 2012.

[2] M. Hämäläinen, T. Paso, L. Mucchi, M. Girod-Genet, J. Farserotu, H. Tanaka, W. H. Chin, and L. N. Ismail, "ETSI TC SmartBAN: Overview of the wireless body area network standard," in *Proc. Int. Symp. Med. Inf. Commun. Technol. (ISMICT)*, May 2015, pp. 1–5, doi: 10.1109/ISMICT.2015.7107485.

[3] M. Chen, S. Gonzalez, A. Vasilakos, H. Cao, and V. C. M. Leung, "Body area networks: A survey," *Mobile Netw. Appl.*, vol. 16, no. 2, pp. 171–193, Apr. 2011, doi: 10.1007/s11036-010-0260-8.

[4] D. Fischer, R. Schreiber, D. Levi, and R. Eliakim, "Capsule endoscopy: The localization system," *Gastrointestinal Endoscopy Clinics North Amer.*, vol. 14, no. 1, pp. 25–31, Jan. 2004, doi: 10.1016/j.giec.2003.10.020.

[5] K. Pahlavan, G. Bao, Y. Ye, S. Makarov, U. Khan, P. Swar, D. Cave, A. Karellas, P. Krishnamurthy, and K. Sayrafian, "RF localization for wireless video capsule endoscopy," *Int. J. Wireless Inf. Netw.*, vol. 19, no. 4, pp. 326–340, Dec. 2012, doi: 10.1007/s10776-012-0195-z.

[6] T. Otim, A. Bahillo, L. E. Diez, P. Lopez-Iturri, and F. Falcone, "Impact of body wearable sensor positions on UWB ranging," *IEEE Sensors J.*, vol. 19, no. 23, pp. 11449–11457, Dec. 2019, doi: 10.1109/JSEN.2019.2935634.

[7] K. Wen, K. Yu, and Y. Li, "NLOS identification and compensation for UWB ranging based on obstruction classification," in *Proc. 25th Eur. Signal Process. Conf. (EUSIPCO)*, Aug. 2017, pp. 2704–2708, doi: 10.23919/EUSIPCO.2017.8081702.

[8] U. Khan, S. N. Makarov, Y. Ye, R. Fu, P. Swar, and K. Pahlavan, "Review of computational techniques for performance evaluation of RF localization inside the human body," *IEEE Rev. Biomed. Eng.*, vol. 12, pp. 123–137, Apr. 2019, doi: 10.1109/RBME.2018.2826535.

[9] M. Barbi, S. Perez-Simbor, C. Garcia-Pardo, C. Andreu, and N. Cardona, "Localization for capsule endoscopy at UWB frequencies using an experimental multilayer phantom," in *Proc. IEEE Wireless Commun. Netw. Conf. Workshops (WCNCW)*, Apr. 2018, pp. 390–395, doi: 10.1109/WCNCW.2018.8369015.

[10] M. Kawasaki and R. Kohno, "Position estimation method of medical implanted devices using estimation of propagation velocity inside human body," *IEICE Trans. Commun.*, vol. E92.B, no. 2, pp. 403–409, 2009, doi: 10.1587/transcom.E92.B.403.

[11] T. Ito, D. Anzai, and J. Wang, "Performance evaluation on RSSI-based wireless capsule endoscope location tracking with particle filter," *IEICE Trans. Commun.*, vol. E97.B, no. 3, pp. 579–586, 2014, doi: 10.1587/transcom.E97.B.579.

[12] T. Ito, T. Iida, D. Anzai, and J. Wang, "An EM imaging-based localization method with sparse reconstruction for implant devices," in *Proc. 38th Annu. Int. Conf. IEEE Eng. Med. Biol. Soc. (EMBC)*, Aug. 2016, pp. 239–242, doi: 10.1109/EMBC.2016.7590684.

[13] T. Iida, D. Anzai, and J. Wang, "Performance evaluation on GA-based localization for wireless capsule endoscope using scattered electric fields," *IEICE Trans. Commun.*, vol. E99.B, no. 3, pp. 578–585, 2016, doi: 10.1587/transcom.2015MIP0002.

[14] R. Penrose, "A generalized inverse for matrices," *Math. Proc. Cambridge Phil. Soc.*, vol. 51, no. 3, pp. 406–413, Jul. 1955, doi: 10.1017/S0305004100030401.

[15] J. Wang and T. Takagi, "A noninvasive method for dielectric property measurement of biological tissues," *IEICE Trans. Commun.*, vol. E77.B, no. 6, pp. 738–742, 1994.

[16] Y. Liu, Z. Zhan, J.-F. Cai, D. Guo, Z. Chen, and X. Qu, "Projected iterative soft-thresholding algorithm for tight frames in compressed sensing magnetic resonance imaging," *IEEE Trans. Med. Imag.*, vol. 35, no. 9, pp. 2130–2140, Sep. 2016, doi: 10.1109/TMI.2016.2550080.

[17] S. Liu, M. Liu, P. Li, J. Zhao, Z. Zhu, and X. Wang, "SAR image denoising via sparse representation in shearlet domain based on continuous cycle spinning," *IEEE Trans. Geosci. Remote Sens.*, vol. 55, no. 5, pp. 2985–2992, May 2017, doi: 10.1109/TGRS.2017.2657602.

[18] S. Gabriel, R. W. Lau, and C. Gabriel, "The dielectric properties of biological tissues: III. Parametric models for the dielectric spectrum of tissues," *Phys. Med. Biol.*, vol. 41, no. 11, pp. 2271–2293, Nov. 1996, doi: 10.1088/0031-9155/41/11/003.

[19] J. Richmond, "Scattering by a dielectric cylinder of arbitrary cross section shape," *IEEE Trans. Antennas Propag.*, vol. AP-13, no. 3, pp. 334–341, May 1965, doi: 10.1109/TAP.1965.1138427.

[20] D. L. Donoho, "Compressed sensing," *IEEE Trans. Inf. Theory*, vol. 52, no. 4, pp. 1289–1306, Apr. 2006, doi: 10.1109/TIT.2006.871582.

[21] K. Hayashi, M. Nagahara, and T. Tanaka, "A user's guide to compressed sensing for communications systems," *IEICE Trans. Commun.*, vol. E96.B, no. 3, pp. 685–712, 2013, doi: 10.1587/transcom.E96.B.685.

[22] T. Nagaoka, S. Watanabe, K. Sakurai, E. Kunieda, S. Watanabe, M. Taki, and Y. Yamanaka, "Development of realistic high-resolution whole-body voxel models of Japanese adult males and females of average height and weight, and application of models to radio-frequency electromagnetic-field dosimetry," *Phys. Med. Biol.*, vol. 49, no. 1, pp. 1–15, Jan. 2004, doi: 10.1088/0031-9155/49/1/001.

[23] Medtronic. *PillCam SB 3 System*. Accessed: Dec. 17, 2020. [Online]. Available: https://www.medtronic.com/covidien/en-us/products/capsule-endoscopy/pillcam-sb-3-system.html

[24] L. Mucchi and A. Carpini, "Aggregate interference in ISM band: WBANs need cognitivity?" in *Proc. 9th Int. Conf. Cognit. Radio Oriented Wireless Netw. (CROWNCOM)*, 2014, pp. 247–253, doi: 10.4108/icst.crowncom.2014.255775.

[25] O. Lauer, M. Riederer, N. Karoui, R. Vahldieck, E. Keller, and J. Fröhlich, "Characterization of the electromagnetic environment in a hospital," in *Proc. Asia–Pacific Symp. Electromagn. Compat., 19th Int. Zurich Symp. Electromagn. Compat. (APEMC)*, May 2008, pp. 474–477, doi: 10.1109/APEMC.2008.4559915.

[26] N. J. LaSorte, W. J. Barnes, and H. H. Refai, "Characterization of the electromagnetic environment in a hospital and propagation study," in *Proc. IEEE Int. Symp. Electromagn. Compat.*, Aug. 2009, pp. 135–140, doi: 10.1109/ISEMC.2009.5284561.

TAKAHIRO ITO (Member, IEEE) received the B.E., M.E., and Ph.D. degrees from the Nagoya Institute of Technology, Aichi, Japan, in 2013, 2015, and 2017, respectively. Since 2017, he has been an Assistant Professor with the Graduate School of Engineering, Nagoya Institute of Technology. He joined the Graduate School of Information Sciences, Hiroshima City University, as an Assistant Professor, in 2020. He has involved in the research of computational electromagnetics in biology and medical applications.

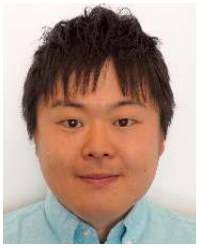

DAISUKE ANZAI (Member, IEEE) received the B.E., M.E., and Ph.D. degrees from Osaka City University, Osaka, Japan, in 2006, 2008, and 2011, respectively. Since 2011, he has been an Assistant Professor with the Graduate School of Engineering, Nagoya Institute of Technology, Nagoya, Japan, where he is currently an Associate Professor. His current research interests include biomedical communication systems and localization systems in wireless communication networks. He was a recipient of the 2015 IEEE MTT-S Japan Young Engineer Award and the Telecommunications Technology Award from the Telecommunications Advancement Foundation.

JIANQING WANG (Fellow, IEEE) received the B.E. degree in electronic engineering from the Beijing Institute of Technology, Beijing, China, in 1984, and the M.E. and D.E. degrees in electrical and communication engineering from Tohoku University, Sendai, Japan, in 1988 and 1991, respectively. He was a Research Associate with Tohoku University, and a Senior Engineer with Sophia Systems Company Ltd. He joined the Nagoya Institute of Technology, Nagoya, Japan, in 1997, where he has been a Professor, since 2005. He has authored *Body Area Communications* (Wiley-IEEE, 2012). His current research interests include biomedical communications and electromagnetic compatibility.

HIROKAZU TAKANA (Senior Member, IEEE) received the B.E. and Ph.D. degrees in communications engineering from Osaka University, Suita, in 1989 and 2001, respectively, and the Ph.D. degree in information sciences from Hokkaido University, Sapporo, in 2015. He joined Toshiba Corporation, as a Researcher, in 1989. From 2007 to 2009, he was a Visiting Researcher with Hokkaido University. From 2007 to 2008, he was a Visiting Associate Professor with Hokkaido University. From 2013 to 2015, he was a Visiting Associate Professor with Yokohama National University. Since 2015, he has been a Professor with Hiroshima City University. Since 1997, he has been involved with international standardization activities in the field of mobile multimedia systems in ITU-T, 3GPP, 3GPP2, and bluetooth. He actively contributed to defining technical specifications of video telephony systems, multimedia streaming systems, multimedia messaging systems, and so on for 3rd-generation wireless communication systems. His research interests include theory and applications of modulation, error control coding, access control and audio/video coding, with emphasis on applications to mobile multimedia communications, broadcasting and dependable wireless communications, and body area network for the IoT systems. He received the ITU-AJ Award from the ITU Association of Japan, in 1999. Since 2013, he has been serving as the Vice Chair for TC Smart BAN in European Telecommunications Standards Institute (ETSI). Since 2015, he serves as the Convener of WG 1 (User Focus) for International Electrotechnical Commission (IEC) Systems Committee Active Assisted Living (SyC. AAL).